Contemporary Mathematics
https://ojs.wiserpub.com/index.php/CM/

Research Article

Chaotic Dynamics in the Cheeger Problem: A Focus on Rectangular Geometries

Praveen Kumar Kushwaha, Lakshmi Narayan Mishra*

Department of Mathematics, School of Advanced Sciences, Vellore Institute of Technology, Vellore, Tamil Nadu, 632014, India
E-mail: lakshminarayanmishra04@gmail.com

Received: 2 August 2025; **Revised:** 9 September 2025; **Accepted:** 17 September 2025

Abstract: This paper presents a novel investigation into the dynamics of the Cheeger problem for rectangular domains. The study introduces a new framework by defining the dynamical system associated with the classical Cheeger problem specifically for rectangular shapes. A key finding is that the conditions $m < 0$ and $q > m$ are sufficient for chaotic behavior in the dynamical system defined for the Cheeger problem on rectangles. In this context, $b(t) = e^{mt}$ represents one of the time-varying dimensions of the rectangle, and $\varepsilon_b(t) = e^{qt}$ represents the perturbation in the same dimension. The maximal deterministic Lyapunov exponent is rigorously derived, showing that chaos emerges as one rectangle dimension decays while perturbations grow. Numerical illustrations confirm chaos onset at finite times $t = 0.2383$ and $t = 0.2494$, demonstrating exponential divergence of trajectories and sensitive dependence on initial conditions. These results establishing fundamental limits on the predictability horizon and enabling precise timing for interventions, thereby bridging theoretical insights with practical foresight and control. Sensitivity analysis further reveals that increasing q accelerates chaos onset, while increasing m stabilizes the system. Altogether, the work advances both theoretical understanding and practical insights into geometric dynamics for complex systems.

***Keywords*:** chaos phenomena, classical Cheeger problem, dynamical system, Lyapunov exponent, rectangular shape

MSC: 37L30, 37N35, 34D08, 37F40

1. Introduction

In geometry, chaotic behavior describes the erratic and intricate patterns that, in specific circumstances, can appear in geometric systems. A characteristic of chaos, this phenomenon frequently occurs in dynamical systems where slight modifications to the initial conditions produce wildly disparate results [1–5]. The evolution of shapes, curves, and surfaces often observed in fractals or in the study of intricate geometric structures can exhibit this behavior in geometric contexts. For example, complex patterns like tree branching or crystal growth can result from the interaction of chaotic motion and geometric constraints. Since it helps to capture the inherent complexities of systems influenced by nonlinear dynamics, an understanding of chaotic behavior in geometry is essential for modeling real-world processes. This allows for deeper insights into a variety of fields, including biology, engineering, and physics. Numerous applications exist for chaotic behavior in geometry [6–11]. By dividing a given domain into two disjoint subsets, the classical Cheeger problem is a

DOI: https://doi.org/10.37256/cm.6620258110

geometric optimization problem that seeks to minimize the ratio of the boundary surface area to the total volume of the subsets [12–17]. It specifically looks for a partition that captures the efficiency of the partitioning by striking a balance between the volume of the subsets and the size of the boundary. We have a great deal of information and proven results about the Cheeger problem for convex sets, but much less for non-convex sets. Please see the references [18–20] for more information.

On the other hand, the generalized Cheeger problem takes into account more complicated situations, like non-homogeneous cases, in which various domain regions might have different weights or properties [21–23]. This leads to a richer and more adaptable framework for geometric optimization by enabling the investigation of partitions that minimize the boundary-to-volume ratio while taking these extra factors into consideration.

The classical Cheeger problem holds significant theoretical and practical importance, demonstrated by its broad applications across various fields such as avalanche and landslide modeling, fracture mechanics, medical imaging, eigenvalue estimation, and capillarity modeling [21, 22, 24–28]. These diverse applications highlight the problems versatility in solving complex scientific and engineering challenges and underscore its role in geometric optimization and nonlinear dynamic systems emerging in nature and technology. Despite extensive existing research, a notable gap remains in thoroughly understanding the chaotic behavior that arises in dynamically evolving geometrical systems governed by the Cheeger framework, particularly in rectangular domains where dimension growth and perturbations critically influence system stability [17, 24–26]. Motivated by this gap, the present study aims to uncover chaos emergence by deriving explicit criteria based on the maximal Lyapunov exponent, thereby bridging geometric analysis with dynamical systems theory and advancing both fields.

1.1 *Contributions of the research paper*

This research is significant for its novel approach in characterizing and rigorously identifying sufficient conditions for chaos onset within the Cheeger problem for rectangular shapes. By establishing the criteria $m < 0$ and $q > m$, the study links geometric evolution directly to chaotic behavior, enabling predictive control through manipulation of dimensional changes and perturbations. This foundational insight enriches theoretical understanding while enabling practical applications, such as forecasting crack dynamics in fracture mechanics, tuning smart materials through controlled chaos, improving hazard prediction in landslide and avalanche modeling, enhancing imaging stability in medical diagnosis, and refining control in engineering systems. Additionally, the study quantifies the minimum prediction horizon for chaos onset (around $t = 0.2383$ and $t = 0.2494$), providing valuable foresight and control timing. Overall, the work fills a critical research gap, introduces novel analytical and numerical methods, and expands the practical and theoretical horizons of the Cheeger problem in complex dynamic systems.

A key finding of this research is that the conditions $m < 0$ and $q > m$ are sufficient for chaotic behavior in the dynamical system defined for the classical Cheeger problem involving rectangular shapes. In this context, $b(t) = e^{mt}$ represents one of the time-varying dimensions of the rectangle, and $\varepsilon_b(t) = e^{qt}$ represents the perturbation in the same dimension. As $m < 0$, this dimension exponentially decays toward zero over time, indicating that one dimension effectively collapses, thereby constraining the state space and potentially increasing sensitivity to initial conditions in the remaining dimensions. Meanwhile, the perturbation $\varepsilon_b(t) = e^{qt}$ grows faster when $q > m$. Because of this dynamic, the state space is constrained by the collapsing dimension, making the other dimensions more sensitive to initial conditions. Chaos is the result of nonlinear interactions being amplified by the interaction between the rapidly growing perturbation and the decaying dimension. Therefore, the conditions $m < 0$ and $q > m$ are in fact sufficient for chaos, highlighting the intricate ways in which dimensionality and perturbations impact the system's complex dynamics. When one dimension is reduced, the available phase space is also reduced, which improves interactions between the other variables and creates an environment that is conducive to chaos. The decaying dimension and intrinsic nonlinearities interact to drive the dynamical system's transition from stability to chaotic behavior over time. This understanding clarifies the mechanisms behind chaotic dynamics and underscores the significance of dimension in influencing the behavior of complex systems. The perturbed dimensions of the rectangle are expressed as $a(t) + \varepsilon_a(t)$ and $b(t) + \varepsilon_b(t)$, where $\varepsilon_a(t)$ and $\varepsilon_b(t)$ are small perturbations, with $a(t) = e^{nt}$, $b(t) = e^{mt}$, $\varepsilon_a(t) = e^{pt}$, and $\varepsilon_b(t) = e^{qt}$. In the main content of the present study, it is theoretically established that such a decaying dimension drives the system toward chaos by yielding a positive maximal

deterministic Lyapunov exponent. However, from a practical perspective, it becomes essential to investigate the specific time interval during which the maximal Lyapunov exponent becomes positive and chaos emerges, while the rectangle still maintains its positive dimensions, thereby preserving its structural integrity. This practical aspect is explored further in the section on numerical illustrations. In the first numerical illustration, it is observed that the system requires a minimum time of $t = 0.2383$ to reach a chaotic state by attaining a positive maximal Lyapunov exponent, while in the second numerical illustration, this minimum time is found to be $t = 0.2494$. Both numerical illustrations, depicted in 1 and 2, clearly exhibit the exponential divergence of nearby trajectories, highlighting the system's Sensitive Dependence on Initial Conditions (SDIC) and strongly suggesting chaotic dynamics. This framework lays the groundwork for further exploration of chaotic dynamics in geometrically constrained systems.

1.2 *Outline of the research paper*

The structure of the paper is organized as follows: Section 2 presents the preliminaries, including recent literature on chaotic dynamics in geometric optimization (Subsection 2.1), a description of J. Cheegers geometrical optimization problem 2.2, and the concept of chaos via the maximal Lyapunov exponent 2.3. Subsections 2.4 to 2.8 review the analytical properties of the classical Cheeger problem for rectangular shapes, which lay the foundation for defining the dynamical system and characterizing chaotic behavior. Section 3 details the main contributions, starting with the research design and methodology 3.1, followed by the formulation of the dynamical system 3.2, derivation of the maximal Lyapunov exponent 3.3, establishing the sufficient condition for chaos 3.4, and its interpretation 3.5. Section 4 covers the numerical techniques 4.1 and provides two numerical illustrations identifying the minimum time for chaos onset while maintaining structural integrity. Section 5 offers a sensitivity analysis of key parameters, Section 6 contains a comparative study, Section 7 discusses results and implications, and Section 8 concludes the paper with future research directions.

2. Preliminaries

In the preliminaries, we concisely describe J. Cheegers geometrical optimization problem [13–15, 18] and the phenomenon of chaos [29–32], together with a brief discussion of the fundamental analytical properties of the classical Cheeger problem for rectangular domains. Although these properties are well established in the literature, they are reviewed here as they are essential for formulating the associated dynamical system and analyzing the onset of chaos. For further details, readers are referred to the cited works. Before proceeding to the main content of this section, we also provide an overview of recent advances in chaotic dynamics within geometric optimization problems.

2.1 *Recent literature on chaotic dynamics in geometric optimization problems*

Recent literature on chaotic dynamics in geometric optimization highlights significant progress in understanding and exploiting chaos for complex problem-solving. Chaos Game Optimization (CGO) algorithms and their variants have been extensively studied, demonstrating effectiveness in binary, multi-objective, and large-scale optimization across domains such as engineering, energy, and machine learning. These studies underscore CGOs adaptability while also identifying challenges such as premature convergence and sensitivity to initial conditions, motivating hybrid algorithms and theoretical improvements [33, 34]. Complementary research explores chaotic dynamics in high-dimensional systems, nonholonomic and infinite-dimensional mechanical models, and geometric control theory, deepening the mathematical understanding of chaos in PDE-constrained and shape optimization problems [35, 36]. Reviews on chaos control provide modern strategies for stabilizing initially unpredictable systems, which are crucial for reliable optimization outcomes. Despite these advances, deterministic analytic frameworks tailored for classical geometric problems, such as the Cheeger problem, remain underdeveloped, particularly in explicitly connecting Lyapunov exponents to evolving geometric parameters, motivating efforts to bridge theory and practical applications [37]. In recent developments on chaotic geometric optimization, fuzzy optimization and functional approximation, particularly their applications in areas such as medical imaging, have emerged as crucial directions [38–43].

Recent theoretical frameworks (2020-2025) emphasize intricate patterns and deterministic laws governing highly sensitive nonlinear systems, where small initial differences amplify exponentially, producing fractals, strange attractors, and spontaneous order. Advances include refined characterizations of chaotic attractors using fractal geometry and Lyapunov exponents, multifaceted bifurcation analyses, and studies of infinite-dimensional and stochastic dynamical systems. There is growing interest in chaos control techniques leveraging feedback and synchronization to stabilize unpredictable systems. Integration of geometric and topological methods, including dynamic Laplacians and supersymmetric theories, has enhanced understanding of chaotic phenomena in PDE-governed systems. Key works include comprehensive reviews on chaos control, and analyses of fractal sequences and convergence behavior, collectively advancing both theoretical rigor and practical strategies for managing chaos in complex geometric and dynamical systems [44, 45].

2.2 *The J. Cheegers geometrical optimization problem*

Let X be an open, non-empty bounded set in $\mathbb{R}^2$. The problem seeks a subset C of the $\mathrm{cl}(X)$ such that the perimeter-to-area ratio of the set C is minimized among all subsets of $\mathrm{cl}(X)$. This ratio is known as the Cheeger constant, denoted by $h(X)$, and the set C that achieves this minimum is referred to as the Cheeger set.

Mathematically, the Cheeger constant can be expressed as:

$$h(X) = \inf_{C \subseteq \mathrm{cl}(X)} \frac{|\partial C|}{|C|}, \tag{1}$$

where:

• $h(X)$ is the Cheeger constant for the set X.

• $|\partial C|$ denotes the perimeter (or boundary measure) of the set C. This is defined as the measure of the boundary points of C.

• $|C|$ is the area (or volume) of the set C, which corresponds to its 2-dimensional Lebesgue measure.

• $\mathrm{cl}(X)$ is the closure of X.

The set C must be smoothly bounded for the Cheeger problem, which means that its boundary must be distinct, continuous, and differentiable. In order to enable meaningful comparisons of the perimeter-to-area ratio, this condition guarantees that the perimeter is well-defined and finite. Rectangular shapes are the specific focus of this study. In this case, the following is an expression for the rectangle's classical Cheeger constant [13]:

$$C(R_{a,\,b}) = \frac{(a+b) + \sqrt{(a-b)^2 + \pi(ab)}}{2ab}. \tag{2}$$

Where $C(R_{a,\,b})$ is the classical Cheeger constant of the rectangle $R_{a,\,b}$ with dimensions a and b.

2.3 *The chaos phenomena*

Chaotic behavior in dynamical systems is characterized by sensitive dependence on initial conditions, meaning that small changes can lead to vastly different outcomes over time. This unpredictability is often quantified using the maximal Lyapunov exponent, which measures the average rate of separation of infinitesimally close trajectories in the system. Mathematically, the maximal Lyapunov exponent λ is defined as [31]:

$$\lambda = \lim_{t \to \infty} \frac{1}{t} \ln \left(\frac{d(t)}{d(0)} \right), \tag{3}$$

where $d(0)$ is the initial distance between two trajectories and $d(t)$ is the distance between them at time t. The natural logarithm, represented by the symbol ln, gives the growth rate in this expression. Trajectories diverge exponentially if $\lambda > 0$ and the system is purely deterministic, exhibiting chaos [31]; if $\lambda < 0$, trajectories converge, indicating stability; and if $\lambda = 0$, the system is usually periodic or quasi-periodic. In order to categorize a system's stability and chaotic features, the maximal Lyapunov exponent is a vital indicator of its dynamical behavior.

2.4 *Analytical framework for chaotic behavior in the Cheeger problem*

The study focuses on establishing a sufficient condition in the dynamics of shape dimensions that enables the existence of chaotic behavior in the classical Cheeger problem. For simplicity, the present work concentrates on rectangular shapes. It is important to highlight the basic requirements for defining the dynamical system and demonstrating chaotic behavior in the classical Cheeger problem, namely the well-definedness, continuity, and differentiability of the Cheeger constant function for rectangular shapes, which are already established in the literature.

2.5 *Well-definedness of the Cheeger constant function for rectangular shape*

Let $C : D \to B$ be the function defined as follows:

$$C(R_{a,\,b}) = \frac{(a+b) + \sqrt{(a-b)^2 + \pi(ab)}}{2ab}. \tag{4}$$

Where $C(R_{a,\,b})$ is the classical Cheeger constant of the rectangle $R_{a,\,b}$ with dimensions a and b.
The domain D of the function is defined as:

$$D = \{(a,\, b) \in \mathbb{R}^2 \mid a > 0,\, b > 0\}. \tag{5}$$

The range set $S \subset B$ is defined as:

$$S = \{C(R_{a,\,b}) \in \mathbb{R} \mid (a,\, b) \in D\}. \tag{6}$$

To prove that the function is well-defined, we need to demonstrate that for every element in the domain D, there is an unique association in the co-domain B.

2.6 *Uniqueness property*

It is trivial to show that $C(R_{a,\,b})$ provides a unique value for each $(a,\, b) \in D$, by establishing:

$$(a_1,\, b_1) = (a_2,\, b_2) \implies C(R_{a_1,\,b_1}) = C(R_{a_2,\,b_2}). \tag{7}$$

Where $(a_1,\, b_1)$ and $(a_2,\, b_2)$ are taken arbitrarily from set D.
Now,

$$C(R_{a_1,\,b_1}) = \frac{(a_1+b_1)+\sqrt{(a_1-b_1)^2+\pi(a_1b_1)}}{2a_1b_1}. \tag{8}$$

$$C(R_{a_2,\,b_2}) = \frac{(a_2+b_2)+\sqrt{(a_2-b_2)^2+\pi(a_2b_2)}}{2a_2b_2}. \tag{9}$$

$\Longrightarrow$

$$\frac{(a_1+b_1)+\sqrt{(a_1-b_1)^2+\pi(a_1b_1)}}{2a_1b_1} = \frac{(a_2+b_2)+\sqrt{(a_2-b_2)^2+\pi(a_2b_2)}}{2a_2b_2}.$$

Since,

$$(a_1,\,b_1) = (a_2,\,b_2). \tag{10}$$

Therefore,

$$C(R_{a_1,\,b_1}) = C(R_{a_2,\,b_2}). \tag{11}$$

2.7 *The continuity property of the classical Cheeger constant function for rectangular shape*

To prove continuity, we observe that $C(R_{a,\,b})$ is composed of continuous functions. Specifically:

• The functions $a+b$, ab, and $(a-b)^2$ are all polynomials in a and b, which are continuous.

• The square root function $\sqrt{x}$ is continuous for $x \geq 0$.

Since the combination of continuous functions (addition, multiplication, and square root) is continuous, $C(R_{a,\,b})$ is continuous for $a,\,b > 0$.

2.8 *The differentiability property of the classical Cheeger constant function for rectangular shape*

To show that $C(R_{a,\,b})$ is differentiable, we compute the partial derivatives with respect to a and b. Using the quotient rule and chain rule, we have:

$$C(R_{a,\,b}) = \frac{(a+b)+\sqrt{(a-b)^2+\pi(ab)}}{2ab}. \tag{12}$$

Let $f(a,\,b) = (a+b)+\sqrt{(a-b)^2+\pi(ab)}$ and $g(a,\,b) = 2ab$.

The derivatives $\dfrac{\partial f}{\partial a}$ and $\dfrac{\partial g}{\partial a}$ can be computed, and similar steps can be taken for b.

• The partial derivative $\dfrac{\partial C}{\partial a}$ is:

$$\frac{\partial C}{\partial a} = \frac{g\dfrac{\partial f}{\partial a} - f\dfrac{\partial g}{\partial a}}{g^2}. \tag{13}$$

• The partial derivative $\dfrac{\partial C}{\partial b}$ is:

$$\frac{\partial C}{\partial b} = \frac{g\dfrac{\partial f}{\partial b} - f\dfrac{\partial g}{\partial b}}{g^2}. \tag{14}$$

$f(a,\ b) = (a+b) + \sqrt{(a-b)^2 + \pi(ab)}$ is not differentiable at (0, 0) due the presence of square root. Thus, the present study exclude the origin (0, 0) and its vicinity from the domain D for the analysis. Let D^* denotes the domain D after deleting the origin (0, 0) and its vicinity. Since f and g are continuously differentiable functions in domain D^*, the partial derivatives of C with respect to a and b exist and continuous respectively, proving $C(R_{a,\ b})$ is differentiable in D^*.

3. The sufficient condition in the dynamics of shape dimensions for the existence of chaotic behaviour in the classical Cheeger problem

The study focuses on establishing a sufficient condition within the dynamics of shape dimensions that enables the emergence of chaotic behavior in the classical Cheeger problem. For simplicity, the present work concentrates on rectangular shapes. The main content begins by formulating the dynamical system corresponding to the classical Cheeger problem for rectangular shapes. Subsequently, it derives an explicit expression for the maximal Lyapunov exponent of the defined system. Finally, the study articulates a sufficient condition for chaos in this dynamical system by invoking the well-established criterion for chaotic behavior, namely $L > 0$, where L denotes the deterministic Lyapunov exponent. Before delving into the main results, we briefly outline the research design and methodology.

3.1 *Research design and methodology*

In classical approaches to computing the maximal Lyapunov exponent of a dynamical system, a large ensemble of pairs of infinitesimally close trajectories is typically considered, and the average rate of separation in the phase space is computed. This strategy ensures the identification of at least one trajectory pair exhibiting exponential divergence, which is crucial for detecting chaotic behavior. In the present study, however, due to the difficulty of explicitly obtaining full trajectories in the phase space, the maximal Lyapunov exponent is evaluated using a single pair of infinitesimally close trajectories. Specifically, leveraging the expression of the Cheeger constant $C(R_{a,\ b})$ of a rectangle in terms of its time-dependent dimensions $a(t)$ and $b(t)$, two neighboring trajectories are considered: $C(R_{a(t),\ b(t)})$ and $C(R_{a(t)+\varepsilon_a(t),\ b(t)+\varepsilon_b(t)})$, where $\varepsilon_a(t)$ and $\varepsilon_b(t)$ denote infinitesimal perturbations in the respective dimensions. The unperturbed and perturbed functions are systematically constructed, often using exponential forms, to maximize the likelihood of observing chaotic behavior, characterized by a positive deterministic Lyapunov exponent. Preliminary observations indicate that exponential forms of the dimension functions effectively facilitate this behavior, as evidenced by the limiting behavior of the maximal Lyapunov exponent.

All simulations are performed using MATRIX LABORATORY program 25.2.0.3042426 (R2025b). The sufficient conditions for chaos are first derived analytically by employing inequalities based on the positivity of the Lyapunov exponent. For numerical evaluation, exact parameter values for m, q, and other system variables are substituted into the Lyapunov exponent formula. The minimum time to chaos is then computed using MATLAB's robust numerical solvers along with custom scripts. To ensure reproducibility, explicit pseudocode outlining the computational process is provided

within the *Numerical Illustration* and *Sensitivity Analysis* sections of the paper, allowing other researchers to verify results or extend the analysis systematically.

3.2 *Dynamical system formulation in the classical Cheeger problem for rectangular shape*

Generally speaking, a dynamical system is any physical or artificial system where an output variable is dependent on one or more input variables and reacts appropriately to changes in the input variables. Dynamical systems are usually studied to comprehend the qualitative and quantitative behavior of the system over time, i.e., how the system's state changes over time. Ordinary Differential Equations (ODEs), which specify the evolution of state variables in phase space, are frequently used in mathematics to characterize dynamical systems. The dynamical system of the classical Cheeger constant for a rectangle whose dimensions vary over time is inferred in this subsection. The Cheeger constant is a key quantity that characterizes the optimal ratio of boundary length to area for subsets of a geometric shape. In our context, we focus on a rectangle defined by $R_{a(t),\, b(t)} = (-b(t),\ b(t)) \times (-a(t),\ a(t))$, where $a(t)$ and $b(t)$ are time-dependent variables representing the height and width of the rectangle, respectively.

We define the Cheeger constant of a rectangle with time-dependent dimensions as a function $C : \mathbb{R}^2 \to \mathbb{R}$, given by

$$C(R_{a(t),\, b(t)}) = \frac{a(t) + b(t) + \sqrt{(a(t) - b(t))^2 + \pi\, a(t)\, b(t)}}{2\, a(t)\, b(t)}, \tag{15}$$

where, $t \in [0,\ \infty]$.

The Cheeger constant function, governed by the time evolution of the rectangle's dimensions, defines the corresponding dynamical system. The minimum number of variables required to uniquely determine the state of this system is the set of time-dependent state variables $a(t)$ and $b(t)$, which represent the dimensions of the rectangle. Accordingly, the phase space of the system is defined as

$$S = \{(a,\ b) : a > 0,\ b > 0\}. \tag{16}$$

The evolution of the system in phase space is governed by the following set of ordinary differential equations:

$$\dot{a} = f_1(a,\ b), \quad \dot{b} = f_2(a,\ b). \tag{17}$$

Where, f_1 and f_2 are some functions dependent on the Cheeger constant function.

The time evolution of the Cheeger constant in phase space is given by the total derivative of the Cheeger constant function with respect to time:

$$\dot{C} = \frac{\partial C}{\partial a} \cdot \dot{a} + \frac{\partial C}{\partial b} \cdot \dot{b}. \tag{18}$$

Where the notations $\dot{a}$, $\dot{b}$, and $\dot{C}$ denote the time derivatives of $a(t)$, $b(t)$, and $C(R_{a(t),\, b(t)})$, respectively. The set of equation numbers (15)-(18) defines the dynamical system in the classical Cheeger problem for the rectangular shape.

3.3 *Maximal lyapunov exponent for the dynamical system defined in Cheeger problem for the rectangle*

To investigate chaotic behavior in the classical Cheeger problem for rectangular shapes, we analyze how the Cheeger constant varies with the dimensions of the rectangle. By manipulating the dynamics of $a(t)$ and $b(t)$, we can explore the conditions under which the system exhibits sensitivity to initial conditions, characterized by a positive Lyapunov exponent. This analysis enhances our understanding of the interplay between geometry and dynamics in the context of the Cheeger constant, emphasizing chaotic behavior as a fundamental aspect of the dynamical system associated with the classical Cheeger problem. Furthermore, by examining the conditions that give rise to chaos, we contribute to a deeper understanding of the classical Cheeger problem within the realm of dynamical systems. We define the maximal Lyapunov exponent λ in relation to the evolution of the Cheeger constant $C(R_{a(t),\, b(t)})$, where the Lyapunov exponent quantifies the rate of separation of infinitesimally close trajectories in the dynamical system defined by the time-dependent dimensions $a(t)$ and $b(t)$.

The maximal Lyapunov exponent is defined as:

$$\lambda = \lim_{t\to\infty} \frac{1}{t} \log\left(\frac{d_t}{d_0}\right). \tag{19}$$

Where,

• d_t is the distance between two trajectories after t seconds.

• d_0 is the initial distance between the two trajectories.

The necessary and sufficient condition for the existence of chaotic behavior in a dynamical system is that the Lyapunov exponent is positive and purely deterministic. In equation number (19), d_0 is a fixed small positive real number. Thus, we can rewrite the expression as:

$$\lambda = \lim_{t\to\infty} \frac{1}{t} \log(d_t) - \lim_{t\to\infty} \frac{1}{t} \log(d_0). \tag{20}$$

Since d_0 is constant, as t approaches infinity, $\frac{1}{t}\log(d_0)$ tends to zero. Then, the equation number (19) becomes:

$$\lambda = \lim_{t\to\infty} \frac{1}{t} \log(d_t). \tag{21}$$

In order to derive the expression for the maximal Lyapunov exponent of the dynamical system defined for the Cheeger problem for the rectangle, we proceed by perturbing the dimensions $a(t)$ and $b(t)$. Specifically, we let the perturbed dimensions be represented as $a(t)+\varepsilon_a(t)$ and $b(t)+\varepsilon_b(t)$, where $\varepsilon_a(t)$ and $\varepsilon_b(t)$ are small perturbations. The evolution of the Cheeger constant can then be expressed in terms of these perturbed dimensions, resulting in an evolution equation that captures how sensitive the Cheeger constant is to changes in the rectangle's dimensions. This framework allows us to analyze the dynamical behavior of the Cheeger constant, revealing the intricate relationship between geometric variations and the resulting dynamical properties of the system.

Thus, we can express the maximal Lyapunov exponent in the context of the Cheeger problem for rectangular shape as follows:

$$\lambda = \lim_{t\to\infty} \frac{1}{t} \log\left(\frac{C(R_{a(t)+\varepsilon_a(t),\, b(t)+\varepsilon_b(t)}) - C(R_{a(t),\, b(t)})}{C(R_{a(0)+\varepsilon_a(0),\, b(0)+\varepsilon_b(0)}) - C(R_{a(0),\, b(0)})}\right). \tag{22}$$

The Cheeger constant for the rectangle $R_{a(t),\, b(t)}$ is given by:

$$C(R_{a(t),\, b(t)}) = \frac{a(t)+b(t)+\sqrt{(a(t)-b(t))^2+\pi a(t)b(t)}}{2a(t)b(t)}. \tag{23}$$

Perturbed Cheeger Constant after t seconds:

$$C(R_{a(t)+\varepsilon_a(t),\, b(t)+\varepsilon_b(t)}) = \frac{N_1+N_2}{D_1}. \tag{24}$$

Where,

$$N_1 = (a(t)+\varepsilon_a(t))+(b(t)+\varepsilon_b(t)), \tag{25}$$

$$N_2 = \sqrt{((a(t)+\varepsilon_a(t))-(b(t)+\varepsilon_b(t)))^2+\pi(a(t)+\varepsilon_a(t))(b(t)+\varepsilon_b(t))}, \tag{26}$$

$$D_1 = 2(a(t)+\varepsilon_a(t))(b(t)+\varepsilon_b(t)). \tag{27}$$

Unperturbed Cheeger Constant after t seconds:

$$C(R_{a(t),\, b(t)}) = \frac{a(t)+b(t)+\sqrt{(a(t)-b(t))^2+\pi a(t)b(t)}}{2a(t)b(t)}. \tag{28}$$

Initial Perturbed Cheeger Constant:

$$C(R_{a(0)+\varepsilon_a(0),\, b(0)+\varepsilon_b(0)}) = \frac{N_3+N_4}{D_2}. \tag{29}$$

Where,

$$N_3 = (a(0)+\varepsilon_a(0))+(b(0)+\varepsilon_b(0)), \tag{30}$$

$$N_4 = \sqrt{((a(0)+\varepsilon_a(0))-(b(0)+\varepsilon_b(0)))^2+\pi(a(0)+\varepsilon_a(0))(b(0)+\varepsilon_b(0))}, \tag{31}$$

$$D_2 = 2(a(0)+\varepsilon_a(0))(b(0)+\varepsilon_b(0)). \tag{32}$$

Initial unperturbed Cheeger Constant:

$$C(R_{a(0),\, b(0)}) = \frac{a(0)+b(0)+\sqrt{(a(0)-b(0))^2+\pi a(0)b(0)}}{2a(0)b(0)}. \tag{33}$$

The maximal Lyapunov exponent for the classical Cheeger problem with rectangular shapes can now be computed by replacing the perturbed Cheeger constant, unperturbed Cheeger constant, initial perturbed Cheeger constant, and initial unperturbed Cheeger constant with the expressions provided by equation (22). The distance between trajectories is then assessed using the Euclidean norm.

3.4 *Deriving the sufficient conditions*

To derive the sufficient condition for the existence of chaotic behavior in the present dynamical system, we construct the dynamics of both the perturbed and unperturbed trajectories associated with the classical Cheeger constant, equivalently defined through the functions $a(t)$, $b(t)$, $\varepsilon_a(t)$, and $\varepsilon_b(t)$, in such a way as to ensure a positive Lyapunov exponent λ, which, in the present case, is purely deterministic.

Analyzing the expression for λ, we note that the exponential function inherently supports the condition $\lambda > 0$. For this purpose, we can set $a(t) = e^{nt}$, $b(t) = e^{mt}$, $\varepsilon_a(t) = e^{pt}$, and $\varepsilon_b(t) = e^{qt}$, where $(n,\, m,\, p,\, q) \in \mathbb{Z}^4$.

By substituting these forms into the limit expression for λ, we can derive sufficient conditions on the parameters n, m, p, and q that facilitate the positivity of λ. This analysis reveals how the growth rates of the dimensions and their perturbations directly influence the dynamical behavior of the Cheeger constant, ultimately demonstrating the potential for chaotic dynamics in this system.

The maximal Lyapunov exponent is defined by equation (21):

$$\lambda \;=\; \lim_{t\to\infty} \frac{1}{t} \log(d_t), \tag{34}$$

where

$$d_t \;=\; C\big(R_{a(t)+\varepsilon_a(t),\, b(t)+\varepsilon_b(t)}\big) - C\big(R_{a(t),\, b(t)}\big), \tag{35}$$

and $C(\cdot)$ denotes the Cheeger constant of a rectangle.

The Cheeger constant of the rectangle with perturbed dimensions:

$$C\big(R_{a(t)+\varepsilon_a(t),\, b(t)+\varepsilon_b(t)}\big) = \frac{N_1+N_2}{D_1}, \tag{36}$$

where,

$$N_1 := (a(t)+\varepsilon_a(t)) + (b(t)+\varepsilon_b(t)),$$

$$N_2 := \sqrt{\big((a(t)+\varepsilon_a(t)) - (b(t)+\varepsilon_b(t))\big)^2 + \pi\,(a(t)+\varepsilon_a(t))(b(t)+\varepsilon_b(t))},$$

$$D_1 := 2\,(a(t)+\varepsilon_a(t))(b(t)+\varepsilon_b(t)).$$

The Cheeger constant of the rectangle with unperturbed dimensions:

$$C\big(R_{a(t),\,b(t)}\big) = \frac{N_3 + N_4}{D_2}, \tag{37}$$

where,

$$N_3 := a(t) + b(t),\; N_4 := \sqrt{(a(t) - b(t))^2 + \pi\, a(t)b(t)},\; D_2 := 2\, a(t)b(t). \tag{38}$$

Thus one may write

$$\lambda = \lim_{t\to\infty} \frac{1}{t} \log\left(\frac{N_1 + N_2}{D_1} - \frac{N_3 + N_4}{D_2} \right). \tag{39}$$

$$\text{Let } E \;=\; \frac{N_1 + N_2}{D_1} - \frac{N_3 + N_4}{D_2} = \frac{\left(\frac{D_2}{2}\right)(N_1 + N_2) - \left(\frac{D_1}{2}\right)(N_3 + N_4)}{\frac{1}{2} D_1 D_2}. \tag{40}$$

By setting

$$a(t) = e^{nt}, \quad b(t) = e^{mt}, \quad \varepsilon_a(t) = e^{pt}, \quad \varepsilon_b(t) = e^{qt}, \quad (n,\, m,\, p,\, q) \in \mathbb{Z}^4, \tag{41}$$

into the expression for E, we obtain the following representation of the Lyapunov exponent λ:

$$\lambda = \lim_{t\to\infty} \frac{1}{t} \log\left(\frac{N_5 - N_6}{D_3} \right). \tag{42}$$

Where,

$$N_5 = e^{nt} e^{mt} \left((e^{nt} + e^{pt}) + (e^{mt} + e^{qt}) + \sqrt{((e^{nt} + e^{pt}) - (e^{mt} + e^{qt}))^2 + \pi (e^{nt} + e^{pt})(e^{mt} + e^{qt})} \right), \tag{43}$$

$$N_6 = (e^{nt} + e^{pt})(e^{mt} + e^{qt}) \left(e^{nt} + e^{mt} + \sqrt{(e^{nt} - e^{mt})^2 + \pi e^{nt} e^{mt}} \right), \tag{44}$$

$$D_3 = 2(e^{nt} + e^{pt})(e^{mt} + e^{qt}) e^{nt} e^{mt}. \tag{45}$$

We solve for the Lyapunov exponent λ by factoring out the dominant exponential term, taking the limit $t \to \infty$, and simplifying the resulting expression; this step-by-step asymptotic factorization provided below to establish the sufficient conditions:

Step 1 Define the dominant exponents

$$k_2 := \max\{n,\ p\}, \quad k_3 := \max\{m,\ q\}, \quad k_4 := \max\{n,\ m\}.$$

Step 2 Factor dominant exponentials in pairwise sums. For large t,

$$e^{nt} + e^{pt} = e^{k_2 t}\left(e^{(n-k_2)t} + e^{(p-k_2)t}\right) \sim e^{k_2 t},$$

$$e^{mt} + e^{qt} = e^{k_3 t}\left(e^{(m-k_3)t} + e^{(q-k_3)t}\right) \sim e^{k_3 t}.$$

Step 3 Inside the square-root terms in N_6, factor the dominant exponent:

$$\left((e^{nt} + e^{pt}) - (e^{mt} + e^{qt})\right)^2 + \pi(e^{nt} + e^{pt})(e^{mt} + e^{qt}) \sim \left(e^{k_2 t} - e^{k_3 t}\right)^2 + \pi e^{k_2 t} e^{k_3 t}.$$

Hence the square root itself scales like $e^{\max\{k_2,\ k_3\}t}$.
Step 4 Factor the leading exponential from N_5:

$$N_5 \sim e^{(n+m)t} \cdot e^{\max\{k_2,\ k_3\}t} = e^{(n+m+\max\{k_2,\ k_3\})t}.$$

Step 5 Factor the leading exponential from N_6:

$$(e^{nt} + e^{pt})(e^{mt} + e^{qt}) \sim e^{(k_2+k_3)t}, \quad e^{nt} + e^{mt} + \sqrt{(e^{nt} - e^{mt})^2 + \pi e^{nt} e^{mt}} \sim e^{k_4 t}.$$

Thus

$$N_6 \sim e^{(k_2+k_3+k_4)t}.$$

Step 6 Factor the leading exponential from D_3:

$$D_3 \sim 2\, e^{(k_2+k_3)t}\ e^{(n+m)t} = e^{(k_2+k_3+n+m)t} \quad \text{(up to the constant 2)}.$$

Step 7 Form the ratio $(N_5 - N_6)/D_3$:

$$\frac{N_5}{D_3} \sim e^{(\max\{k_2,\ k_3\}-k_2-k_3)t}, \quad \frac{N_6}{D_3} \sim e^{(k_4-n-m)t}.$$

Therefore

$$\frac{N_5 - N_6}{D_3} \sim e^{(\max\{k_2,\, k_3\} - k_2 - k_3)t} - e^{(k_4 - n - m)t}.$$

Step 8 Set $K_1 := \max\{k_2,\, k_3\}$. Then

$$\frac{N_5 - N_6}{D_3} \sim e^{(K_1 - k_2 - k_3)t} - e^{(k_4 - n - m)t}.$$

Step 9 Take the logarithm, divide by t, and pass to the limit:

$$\lambda = \lim_{t\to\infty} \frac{1}{t} \log \left| \frac{N_5 - N_6}{D_3} \right| = \lim_{t\to\infty} \frac{1}{t} \log \left| e^{(K_1 - k_2 - k_3)t} - e^{(k_4 - n - m)t} \right|.$$

This yields equation (46):

$$\lambda \;=\; \lim_{t\to\infty} \frac{1}{t} \log \left| e^{(K_1 - k_2 - k_3)t} - e^{(k_4 - n - m)t} \right|. \tag{46}$$

Evaluation of the limit:
Define

$$\alpha := K_1 - k_2 - k_3, \quad \beta := k_4 - n - m.$$

Then

$$\lambda = \lim_{t\to\infty} \frac{1}{t} \log |e^{\alpha t} - e^{\beta t}|.$$

Case 1: $\alpha > \beta$. Factor $e^{\alpha t}$: $\lambda \to \alpha$.
Case 2: $\beta > \alpha$. Factor $e^{\beta t}$: $\lambda \to \beta$.
Case 3: $\alpha = \beta$. Then $\lambda = \alpha = \beta$, unless cancellation of coefficients occurs, which is nongeneric.
Thus:

$$\lambda = \max\{\alpha,\, \beta\} = \max\{K_1 - k_2 - k_3,\, k_4 - n - m\}.$$

Step-by-step derivation of the sufficient condition for chaos:
Step 1: Assign exponents
Without loss of generality, we choose:

$$K_1 = n, \quad n \geq p \,(\text{so } k_2 = n), \quad q > m \,(\text{so } k_3 = q), \quad n \geq m \,(\text{so } k_4 = n).$$

Step 2: Compute asymptotic coefficients
The Lyapunov exponent depends on the dominant asymptotic terms:

$$\alpha = K_1 - k_2 - k_3 = n - n - q = -q, \quad \beta = K_1 - k_2 - k_4 = n - n - m = -m.$$

Step 3: Identify the maximal exponent
Since $q > m$, we have $-q < -m$, which implies

$$\beta > \alpha.$$

Therefore, the maximal Lyapunov exponent is

$$\lambda = \beta = -m.$$

Step 4: Establish the sufficient condition for chaos
For chaotic behavior, the Lyapunov exponent must be positive:

$$\lambda > 0 \implies -m > 0 \implies m < 0.$$

Additionally, $q > m$ ensures that the perturbation grows faster than the decaying dimension, which is necessary for divergence.

Step 5: Conclude the criterion
Hence, the explicit sufficient conditions for chaotic dynamics are

$$m < 0 \quad \text{and} \quad q > m,$$

with the corresponding maximal Lyapunov exponent

$$\lambda = -m > 0.$$

This establishes both the criterion for chaos and the explicit Lyapunov exponent.

3.5 *The sufficient condition and its interpretation*

The function $b(t) = e^{mt}$ represents one dimension of the rectangle in the context of the classical Cheeger problem for rectangular shapes. It decays exponentially to zero when $m < 0$, whereas the perturbation $\varepsilon_b(t) = e^{qt}$ grows faster when $q > m$. In this case, the state space is constrained by the collapsing dimension, making the remaining dimensions more sensitive to initial conditions. Chaos is the result of nonlinear interactions being amplified by the interaction between the rapidly growing perturbation and the decaying dimension. Theoretically, such a decaying dimension produces a positive deterministic Lyapunov exponent, which pushes the system towards chaos. Practically speaking, though, it becomes crucial to look into the precise moment at which the Lyapunov exponent turns positive and chaos arises while the rectangle

maintains its positive dimensions and its structural integrity. In the section that follows, this practical aspect is further examined using numerical examples.

4. Numerical illustrations

Before proceeding to the numerical illustrations, the present work highlights the numerical technique employed for computing the maximal Lyapunov exponent and determining the precise onset of chaos.

4.1 *Numerical technique*

The numerical methodology centers on computing the maximal Lyapunov exponent:

$$\lambda = \lim_{t\to\infty} \frac{1}{t} \log \frac{d_t}{d_0},$$

where d_t is the separation between perturbed and unperturbed Cheeger constants with time-varying dimensions. Explicit exponential parameterizations for $a(t)$, $b(t)$, $\varepsilon_a(t)$, $\varepsilon_b(t)$ are substituted, and the chaos condition is tested via the function $f(t)$ on a dense temporal grid $[10^{-5},\ 5]$ with fine step $\Delta t = 10^{-6}$. The earliest t satisfying $f(t) > 0$ marks the onset of chaos.

For sensitivity analysis, parameters m and q are varied independently (with the other fixed), each sampled across prescribed intervals. At every sampled value, $f(t)$ is evaluated on the same dense grid to locate the minimum chaos time. Results are compiled, smoothed with spline interpolation, and visualized.

This brute-force yet precise approach-combining analytic parameterization, exhaustive time scanning, and parameter sweeps-ensures robustness, reproducibility, and clear identification of nonlinear sensitivity in chaos onset.

4.2 *Illustration*

Illustration 1:

The Lyapunov exponent is given by:

$$\lambda = \lim_{t\to\infty} \frac{1}{t} \log \left(\frac{d_t}{d_0} \right). \tag{47}$$

Where,

$$d_t = C\left(R_{a(t)+\varepsilon_a(t),\ b(t)+\varepsilon_b(t)}\right) - C\left(R_{a(t),\ b(t)}\right),$$

$$d_0 = C\left(R_{a(0)+\varepsilon_a(0),\ b(0)+\varepsilon_b(0)}\right) - C\left(R_{a(0),\ b(0)}\right),$$

$$C(R_{a,\ b}) = \frac{(a+b) + \sqrt{(a-b)^2 + \pi ab}}{2ab}.$$

Let $a(t) = e^{nt}$, $b(t) = e^{mt}$, $\varepsilon_a(t) = e^{pt}$, $\varepsilon_b(t) = e^{qt}$, where $n = 5$, $m = -1$, $p = -2$, $q = 3$.

Substituting the value of d_0 in (4.1), we get:

$$\lambda = \lim_{t\to\infty} \frac{1}{t} \log\left(\frac{d_t}{0.9431}\right).$$

$$\lambda = \lim_{t\to\infty} \frac{1}{t} \log(d_t) - \lim_{t\to\infty} \frac{1}{t} \log(0.9431).$$

$$\lambda = \lim_{t\to\infty} \frac{1}{t} \log(d_t) + \lim_{t\to\infty} \frac{1}{t} (0.0583).$$

For $\lambda > 0$, we require

$$\log|d_t| + 0.0583 > 0 \implies |d_t| > e^{-0.0583} \implies |d_t| > 0.9433.$$

To determine the first appearance of a positive Lyapunov exponent, we seek the smallest value of t such that

$$|d_t| > 0.9433 \quad \Longleftrightarrow \quad \frac{|N_5 - N_6|}{|D_3|} > 0.9433.$$

The above inequality is solved numerically using MATLAB, yielding $t = 0.2383$. The following presents the algorithm corresponding to the MATLAB implementation:

Algorithm 1 Identification of Minimum Time t for Onset of Chaos in the Dynamical System
Require: Parameters: $n = 5$, $m = -1$, $p = -2$, $q = 3$
Require: Search range: $t_{\min} = 0.00001$, $t_{\max} = 5$, step size $\Delta t = 0.000001$
Ensure: Minimum t such that $f(t) > 0$
1: Define the function $f(t)$ as in Eq. (4.2)
2: Generate values of $t \in [t_{\min},\ t_{\max}]$ with increment Δt
3: **for** each value of t **do**
4: Compute $f(t)$
5: **if** $f(t) > 0$ **then**
6: **return** value of t
7: **end if**
8: **end for**
9: **Report:** No positive value found for $f(t)$ in the given range.

$$f(t) = \left|\frac{M_1 + M_2}{M_3} - \frac{M_4 \cdot M_5}{M_3}\right| - 0.9433 \tag{48}$$

$$M_1 = e^{nt}e^{mt}\left(e^{nt} + e^{pt} + e^{mt} + e^{qt}\right),$$

$$M_2 = \sqrt{\left(e^{nt} + e^{pt} - e^{mt} - e^{qt}\right)^2 + \pi(e^{nt} + e^{pt})(e^{mt} + e^{qt})},$$

$$M_3 = 2(e^{nt} + e^{pt})(e^{mt} + e^{qt})e^{nt}e^{mt},$$

$$M_4 = (e^{nt} + e^{pt})(e^{mt} + e^{qt}), \tag{49}$$

$$M_5 = e^{nt} + e^{mt} + \sqrt{(e^{nt} - e^{mt})^2 + \pi e^{nt}e^{mt}}.$$

The parameter functions in the first numerical example are set as follows: $a(t) = e^{nt}$, $b(t) = e^{mt}$, $\varepsilon_a(t) = e^{pt}$, and $\varepsilon_b(t) = e^{qt}$, where $n = 5$, $m = -1$, $p = -2$, and $q = 3$. At $t = 0.2383$ units of time, we obtain a positive Lyapunov exponent for the first time by putting the sufficient conditions $m < 0$ and $q > m$ into practice. This outcome has practical significance since it shows that chaos will eventually break out in the system. Notably, the system maintains a distinct rectangular structure even as chaos arises, preventing the situation where $t \to \infty$ would cause one of the rectangle's dimensions to collapse. Chaos is the result of nonlinear interactions being amplified by the interaction between the rapidly growing perturbation and the decaying dimension. As a result, the conditions $m < 0$ and $q > m$ are sufficient for chaos, demonstrating the intricate relationship between dimensionality and perturbations and complex dynamics. The conditions $m = -1$ and $q = 3$ together not only demonstrate the existence of chaos but also the complex connection between dimensionality and chaotic behavior, highlighting the crucial role of the Lyapunov exponent in describing the system's stability and complexity. The graph of two adjacent trajectories that diverge exponentially is shown in Figure 1. This shows the system's Sensitive Dependence on Initial Conditions (SDIC), a clear sign of chaotic behavior. The graph is generated using MATLAB software, plotting the Cheeger constant against the time variable, where the x-axis represents time and the y-axis represents the Cheeger constant. The simulation is performed with the parametric values $n = 5$, $m = -1$, $p = -2$, and $q = 3$.

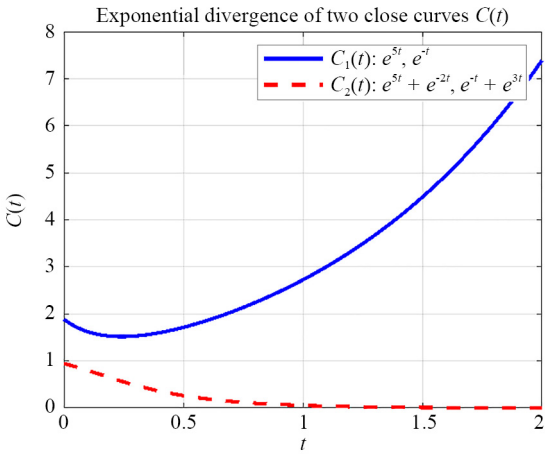

Figure 1. SDIC ($n = 5,\ q = 3$)

Illustration 2:

The Lyapunov exponent is given by:

$$\lambda = \lim_{t\to\infty} \frac{1}{t} \log\left(\frac{d_t}{d_0}\right). \tag{50}$$

Where,

$$d_t = C\left(R_{a(t)+\varepsilon_a(t),\, b(t)+\varepsilon_b(t)}\right) - C\left(R_{a(t),\, b(t)}\right),$$

$$d_0 = C\left(R_{a(0)+\varepsilon_a(0),\, b(0)+\varepsilon_b(0)}\right) - C\left(R_{a(0),\, b(0)}\right),$$

$$C(R_{a,\, b}) = \frac{(a+b)+\sqrt{(a-b)^2+\pi ab}}{2ab}.$$

Let $a(t) = e^{nt}$, $b(t) = e^{mt}$, $\varepsilon_a(t) = e^{pt}$, $\varepsilon_b(t) = e^{qt}$, where $n = 3$, $m = -1$, $p = -2$, $q = 2$.
Substituting the value of d_0 in (4.3), we get:

$$\lambda = \lim_{t\to\infty} \frac{1}{t} \log\left(\frac{d_t}{0.9431}\right).$$

$$\lambda = \lim_{t\to\infty} \frac{1}{t} \log(d_t) - \lim_{t\to\infty} \frac{1}{t} \log(0.9431).$$

$$\lambda = \lim_{t\to\infty} \frac{1}{t} \log(d_t) + \lim_{t\to\infty} \frac{1}{t} (0.0583).$$

To determine the first appearance of a positive Lyapunov exponent, we seek the smallest value of t such that

$$|d_t| > 0.9433 \implies \frac{|N_5 - N_6|}{|D_3|} > 0.9433.$$

The above inequality is solved numerically using MATLAB, yielding $t = 0.2494$. The following presents the algorithm corresponding to the MATLAB implementation:

Algorithm 2 Identification of Minimum Time t for Onset of Chaos in the Dynamical System
Require: Parameters: $n = 3$, $m = -1$, $p = -2$, $q = 2$
Require: Search range: Search range: $t_{\min} = 0.00001$, $t_{\max} = 5$, step size $\Delta t = 0.000001$
Ensure: Minimum t such that $f(t) > 0$
1: Define the function $f(t)$ as in Eq. (4.4)
2: Generate values of $t \in [t_{\min}, t_{\max}]$ with increment Δt
3: **for** each value of t **do**
4: Compute $f(t)$
5: **if** $f(t) > 0$ **then**
6: **return** value of t
7: **end if**
8: **end for**
9: **Report:** No positive value found for $f(t)$ in the given range.

$$f(t) = \left| \frac{M_1 + M_2}{M_3} - \frac{M_4 \cdot M_5}{M_3} \right| - 0.9433 \tag{51}$$

$$M_1 = e^{nt} e^{mt} \left(e^{nt} + e^{pt} + e^{mt} + e^{qt} \right),$$

$$M_2 = \sqrt{(e^{nt} + e^{pt} - e^{mt} - e^{qt})^2 + \pi (e^{nt} + e^{pt})(e^{mt} + e^{qt})},$$

$$M_3 = 2(e^{nt} + e^{pt})(e^{mt} + e^{qt}) e^{nt} e^{mt}, \tag{52}$$

$$M_4 = (e^{nt} + e^{pt})(e^{mt} + e^{qt}),$$

$$M_5 = e^{nt} + e^{mt} + \sqrt{(e^{nt} - e^{mt})^2 + \pi e^{nt} e^{mt}}.$$

In the second numerical illustration, we consider the parametric values $n = 3$, $m = -1$, $p = -2$, and $q = 2$. Here, we maintain the same values for m and p while varying n and q compared to the previous illustration. This combination illustrates how different growth rates in the dimensions governed by n and q can coexist with the decay dictated by m and p. Despite these variations, the consistent negative value of m and the condition $q > m$ remain critical for fostering chaotic dynamics. At $t = 0.2494$ units of time, we obtain a positive Lyapunov exponent for the first time.

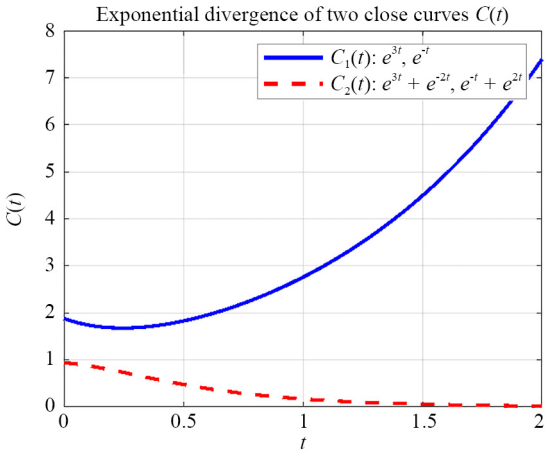

Figure 2. SDIC ($n = 3,\ q = 2$)

This indicates that the fundamental mechanism for chaos remains resilient to variations in the rates at which the other dimensions grow. In addition to supporting our conclusions that the conditions $m = -1$ and $q = 2$ are sufficient for chaos, the flexibility in parameter selection exposes the intricate interaction between different rates of growth and decay in determining the dynamical system's overall behavior. As a result, the system continues to be chaotic, confirming the importance of parameter selection and dimensionality in the development of chaotic behavior. Figure 2 illustrates the graph of two nearby trajectories that diverge exponentially, demonstrating the Sensitive Dependence on Initial Conditions (SDIC) of the system, which is a strong indication of chaotic behavior. The graph is generated using MATLAB software,

plotting the Cheeger constant against the time variable, where the x-axis represents time and the y-axis represents the Cheeger constant. The simulation is performed with the parametric values $n = 3$, $m = -1$, $p = -2$, and $q = 2$.

5. Sensitivity analysis

In the present work on the chaotic onset in the Cheeger problem, a detailed comparative sensitivity analysis between the two key parameters m and q has conducted. Both parameters influence the timing of chaos emergence, but their sensitivities differ in magnitude and nature. The analysis reveals that q tends to have a stronger and more immediate effect on reducing the minimum time to chaos as it increases, indicating a higher sensitivity to variation. In contrast, m exhibits a more stabilizing influence, with increases in m delaying chaos onset, though its sensitivity grows stronger as it approaches critical thresholds near zero from the negative side. This comparative understanding of parameter sensitivities allows for more precise control strategies by prioritizing which parameter adjustments yield more significant impacts on chaotic behavior. Such results align with modern sensitivity approaches in chaotic systems, highlighting the importance of evaluating parameter influence through systematic perturbations and leveraging advanced methods such as adjoint and shadowing-based sensitivity calculations to inform robust design and control in chaotic dynamical systems. Figures 3 and 4 illustrate the relationship between the parameters m and q and the minimum time required for chaos onset, providing clear insights for sensitivity analysis.

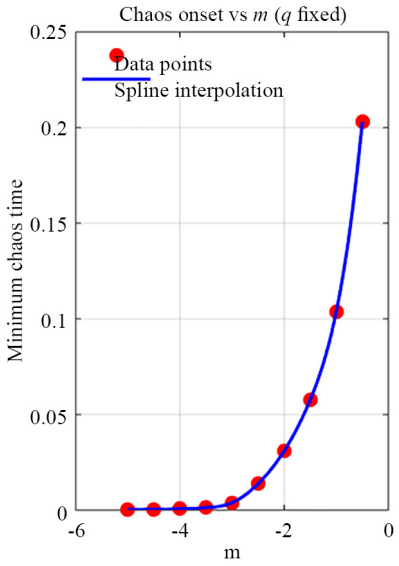

Figure 3. Sensitivity analysis (m vs t)

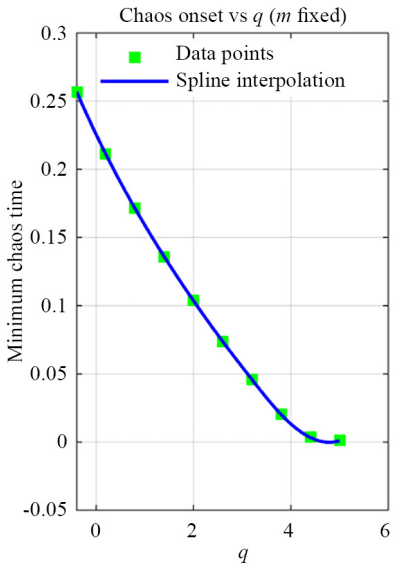

Figure 4. Sensitivity analysis (q vs t)

1. **Chaos Onset vs parameter q (with m fixed):**

• As the parameter q increases from 0 to around 5, the minimum time to chaos decreases sharply from approximately 0.26 to near zero.

• This indicates a strong negative sensitivity of the chaos onset time to increasing q; a higher q accelerates the transition to chaos.

• The curve is nonlinear, with a steep decrease initially which slows down as q increases, reflecting diminishing returns in chaos time reduction for large q.

2. **Chaos Onset vs parameter m (with q fixed):**

• As m increases from -5 towards -0.5, the minimum time to chaos increases from near zero to approximately 0.2.

• This shows a positive sensitivity of chaos onset time to increasing m; as m becomes less negative, the system delays or resists chaos onset.

• The relationship is also nonlinear with rapid changes near $m = -2$ to -1, suggesting sensitive dependence in this parameter region.

Overall sensitivity summary:

• Increasing q reduces the time required for chaos onset, making the system transition to chaos faster.

• Increasing m increases the chaos onset time, effectively stabilizing the system against early chaos.

• Both parameters have a nonlinear impact on chaos timing, with more pronounced sensitivity in certain ranges (q near zero; m near -2 to -1), indicating these regions are critical for control or prediction.

• The graphs confirm the robustness of the chaos onset criteria by showing smooth but sensitive dependency, highlighting the need for careful parameter control to predict or delay chaos in practical applications.

This sensitivity behavior assists in identifying parameter regimes more vulnerable to chaotic transitions and those offering greater stability, essential for design and intervention strategies. The pseudocode for the MATLAB implementation used to generate the graphs depicting the relationship between the parameters m and q and the chaos onset time is provided below to ensure reproducibility of the results.

Algorithm 3 Sensitivity Analysis of Chaos Onset Time for Rectangular Cheeger Systems

Input:

• Parameters: $n = 3$, $p = -2$.

• m range: 10 values in $[-5,\ -0.5]$ (for m-sensitivity, q fixed).

• q range: 10 values in $[-0.2,\ 5]$ (for q-sensitivity, m fixed).

• Fixed parameters: $q_{\text{fixed}} = 2$ for m-sensitivity, $m_{\text{fixed}} = -1$ for q-sensitivity.

• Time range: $t \in [10^{-5},\ 5]$, step $\Delta t = 10^{-5}$.

Output: Minimum chaos onset times $t_{\min}$ for each m and q; interpolated sensitivity curves.

Initialize arrays $t\_results\_m$ and $t\_results\_q$ with NaN values.

for each m in m-values **do**

  Define $f(t) = |d_t| - 0.9433$, using $M_1,\ M_2,\ M_3,\ M_4,\ M_5$ with $(n,\ m,\ p,\ q_{\text{fixed}})$.

  Generate time grid $t = t_{\min} : \Delta t : t_{\max}$.

  Evaluate $f(t)$ at each time point.

  Find first index i such that $f(t_i) > 0$.

  if such index exists **then**

    Record t_i in $t\_results\_m$.

  end if

end for

for each q in q-values **do**

  Define $f(t) = |d_t| - 0.9433$, using $M_1,\ M_2,\ M_3,\ M_4,\ M_5$ with $(n,\ m_{\text{fixed}},\ p,\ q)$.

  Generate time grid $t = t_{\min} : \Delta t : t_{\max}$.

  Evaluate $f(t)$ at each time point.

  Find first index i such that $f(t_i) > 0$.

  if such index exists **then**

    Record t_i in $t\_results\_q$.

  end if

end for

Interpolate and plot results:

• m-sensitivity: plot $(m,\ t\_results\_m)$ and perform spline interpolation.

• q-sensitivity: plot $(q,\ t\_results\_q)$ and perform spline interpolation.

Define helper functions $M_1,\ M_2,\ M_3,\ M_4,\ M_5$ explicitly using exponential expressions of $a(t),\ b(t),\ \varepsilon_a(t),\ \varepsilon_b(t)$.

End of Algorithm.

6. Comparative evaluation: proposed framework vs. contemporary chaos-based optimization

The proposed framework for computing the maximal Lyapunov exponent based on the explicit Cheeger constant of rectangles and a targeted single trajectory pair differs fundamentally from contemporary chaos-based optimization methods, which rely on ensemble averaging, chaotic maps, and statistical estimations in complex phase spaces.

6.1 *Present study*

• **Deterministic Geometry:** Directly exploits the analytic formula for the Cheeger constant in rectangles, with time-dependent side lengths and perturbations defining unperturbed and perturbed trajectories.

• **Single Trajectory Pair:** Evaluates the Lyapunov exponent from one systematically chosen pair of trajectories, instead of ensemble averaging.

• **Analytic Control:** Exponentially varying functions $a(t)$, $b(t)$ and perturbations $\varepsilon_a(t)$, $\varepsilon_b(t)$ allow controlled sensitivity to chaos.

• **Deterministic Lyapunov Exponent:** Computed explicitly from the geometry, unlike statistical or empirical estimates in metaheuristic approaches.

6.2 *Recent chaos-based optimization methods*

• **Statistical Averaging:** Lyapunov exponents estimated from ensemble simulations of chaotic trajectories (e.g., Chaotic Transient Search Optimization (CTSO), Chaotic Runge Kutta Optimization (CRUN), CGO) [46].

• **Algorithmic Complexity:** Depend on chaotic maps (Logistic, Tent, Sine) and population-based randomness without closed-form geometric access [47].

• **Global Search:** Ensemble methods ensure coverage in high-dimensional, nonlinear optimization landscapes [35].

• **Empirical Chaos Detection:** Exponents often used as heuristic indicators of convergence and stability rather than analytic quantities [48].

Table 1. Comparison at a glance between the proposed framework and recent methods

Aspect	Proposed framework	Recent methods (CTSO, CRUN, CGO)
Trajectories	Single, deterministic pair	Ensemble, many averaged pairs
Lyapunov exponent	Explicit, geometry-driven	Empirical, statistical estimate
System type	Rectangular Cheeger (tractable)	Complex, high-dimensional
Chaos induction	Geometric perturbations	Chaotic maps and randomness

In summary, this study advances a deterministic, geometry-based method for chaos detection in the Cheeger problem, clearly distinguished from recent metaheuristic approaches that rely on stochastic ensembles and empirical chaos measures for general nonlinear optimization problems (see Table 1).

7. Results and discussions

7.1 *Novel contribution: dynamical systems approach to the classical Cheeger problem for rectangular domains*

This study introduces a novel framework by defining the dynamical system associated with the classical Cheeger problem specifically for rectangular shapes, emphasizing the fundamental role of geometric characteristics in shaping chaotic dynamics. It rigorously derives the maximal deterministic Lyapunov exponent tied to this system, bypassing stochastic or ensemble methods, and formulates a precise mathematical model quantifying the system's sensitivity to initial conditions through trajectory analysis. The work highlights the pivotal influence of rectangle dimensions on the calculation of the Lyapunov exponent, establishing a direct connection between geometry and global system dynamics. This comprehensive approach not only deepens theoretical understanding of chaos in geometric settings but also pioneers a systematic method to analyze the interplay between shape, dynamics, and stability in complex systems, representing a significant advancement in the study of the Cheeger problem and its dynamic interpretations.

7.2 *Key contributions: sufficient condition and finite-time chaos onset estimation*

A significant result of this research is the identification of the explicit sufficient conditions $m < 0$ and $q > m$ for the emergence of chaotic behavior in the dynamical system defined by the classical Cheeger problem for rectangular domains. Here, the perturbed and unperturbed dimensions are respectively modeled as $a(t) + \varepsilon_a(t) = e^{nt} + e^{pt}$ and $b(t) + \varepsilon_b(t) = e^{mt} + e^{qt}$, with $m < 0$ indicating a dimension decay and $q > m$ indicating a faster-growing perturbation.

This dynamic results in the collapsing dimension constraining the state space and amplifying nonlinear interactions, producing chaos characterized by a positive maximal Lyapunov exponent. Importantly, the study extends these theoretical insights with practical relevance by estimating the minimum finite times $t = 0.2383$ and $t = 0.2494$ at which the maximal Lyapunov exponent becomes positive while the rectangle still maintains positive dimensions, thus preserving structural integrity. These finite-time chaos onset estimates are demonstrated via numerical illustrations showing clear exponential divergence of nearby trajectories, visualized as time-varying Cheeger constants. This combination of established sufficient conditions and finite-time transition quantification provides concrete predictive capability for chaotic transitions in geometric systems, bridging theory and practice, especially in fields where the Cheeger set represents critical structural thresholds, such as fracture mechanics, landslide, and avalanche modeling.

7.3 *Sensitivity analysis of chaos onset with respect to parameters m and q*

In the present work, a comprehensive sensitivity analysis of the chaotic onset in the Cheeger problem has performed, focusing on the parameters m and q, which play distinct roles in influencing the timing of chaos emergence. The analysis reveals that increasing q significantly accelerates chaos onset, exhibiting a strong negative sensitivity where chaos time sharply decreases as q grows, though with diminishing returns for large q. Conversely, the parameter m acts as a stabilizing factor: as m increases from more negative values towards zero, the chaos onset time increases, indicating a positive sensitivity that delays or resists chaos, with heightened sensitivity near the critical range of $[-2, -1]$. These nonlinear dependencies identify critical parameter regions crucial for effective control and prediction. The smooth but sensitive trends shown in Figures 3 and 4 validate the robustness of the proposed chaos onset criteria and emphasize the importance of carefully tuning system parameters to manage chaotic transitions in practical applications. This insight aids in recognizing vulnerable regimes prone to early chaos and those offering greater stability, thus guiding design and intervention strategies in complex dynamical systems.

7.4 *Comparative insights: explicit geometry vs. ensemble-based chaos approaches*

The present framework fundamentally differs from recent chaos-based optimization approaches by replacing statistical and heuristic strategies with a deterministic, geometry-driven method. Instead of relying on ensemble averaging and chaotic maps to estimate Lyapunov exponents, it derives the exponent explicitly from the Cheeger constant of rectangles using a single, carefully chosen trajectory pair. This direct connection to geometry provides analytic precision and computational efficiency, in contrast to the empirical and population-based techniques employed in contemporary methods. While recent approaches are designed for high-dimensional, non-analytic optimization landscapes, the current work exploits the tractable structure of the rectangular Cheeger problem, allowing controlled sensitivity through exponential variations in side lengths and perturbations. By achieving chaos detection without stochastic ensembles, the framework establishes a rigorous and transparent alternative that complements and strengthens the broader landscape of chaos-based methodologies.

7.5 *Practical applications and significance*

The sufficient condition identified in the study, $m < 0$ and $q > m$, provides a critical link between geometric evolution and the onset of chaotic behavior in the Cheeger problem for rectangular shapes, enabling predictive control over chaos through manipulation of dimensional changes and perturbations. This allows designers to establish safe operational thresholds where systems behave predictably or, conversely, to harness chaotic dynamics for beneficial randomness in simulations or materials tuning. Practical applications are wide-ranging: in structural and fracture mechanics, it aids in forecasting when crack growth transitions from stable to chaotic, enabling preemptive reinforcement; in smart materials, it guides programmed transitions between ordered and chaotic states to tune mechanical or thermal properties; for landslide and avalanche modeling, it improves hazard forecasting and early warning by predicting chaotic transitions in evolving terrains; in medical imaging, it enhances segmentation stability by anticipating chaotic boundary shifts; and in engineering control systems, it informs stabilization strategies and refines computational simulations to maintain accuracy up to

chaos thresholds. The study further quantifies the minimum time to chaos (around $t = 0.2383$ and $t = 0.2494$), setting fundamental limits on predictability horizons and enabling precise timing for interventions, thus bridging theoretical understanding with practical foresight and control capabilities.

8. Conclusions and future work

8.1 *Conclusions*

The present study introduces a novel investigation into the dynamics of the Cheeger problem for rectangular domains, establishing a direct connection between geometry and chaotic behavior. By deriving a sufficient condition for chaos, the work demonstrates how the interplay between dimensional evolution and sensitivity to perturbations drives complex dynamical responses. A key contribution is the analytic derivation of the maximal deterministic Lyapunov exponent in the classical Cheeger setting, achieved without reliance on ensemble averages or stochastic approximations. This deterministic framework highlights the pivotal role of rectangle dimensions in governing the onset of chaos, thereby advancing both the mathematical theory of Cheeger sets and their dynamical interpretations. The study further contributes by identifying the precise times $t \approx 0.2383$ and $t \approx 0.2494$ at which the maximal Lyapunov exponent becomes positive, signaling the emergence of chaos while the system maintains its structural integrity. These critical thresholds define practical predictability horizons, enabling timely interventions and linking theoretical chaos characterization to real-world control applications.

The sensitivity analysis underscores how system parameters modulate chaos onset. Specifically, increasing the growth parameter q accelerates the transition to chaos, while increasing m delays it, thereby stabilizing the system against premature instability. The nonlinear dependency of chaos timing on these parameters reveals critical regions, particularly for q near zero and m in the range $[-2,-1]$, which are especially important for control and prediction. Numerical simulations confirm these trends with smooth yet highly sensitive dependency curves, validating the robustness of the analytic chaos onset criteria and demonstrating their practical predictive power.

A comparative perspective places the present work in sharp contrast with recent chaos-based optimization methods. Whereas contemporary approaches rely on statistical averaging, heuristic ensembles, and chaotic maps in high-dimensional optimization landscapes, the current framework leverages explicit geometry and deterministic analysis. By computing the Lyapunov exponent from a single pair of carefully constructed trajectories, the proposed method eliminates the need for stochastic ensembles, providing clarity, analytic precision, and computational efficiency. This distinction situates the present contribution as both rigorous and complementary to existing chaos-based techniques.

Several features and advantages of this approach emerge. The present work establishes the explicit sufficient condition $m < 0$ and $q > m$, which directly links geometric evolution to the onset of chaotic behavior in the classical Cheeger problem for rectangular domains. The derivation of an analytic formula for the maximal Lyapunov exponent facilitates deterministic predictability and yields rare, precise benchmarks for the finite-time transition to chaos (around $t \approx 0.2383$ and $t \approx 0.2494$). Given the well-established role of the Cheeger set as the weakest portion of a domain and its constant as a threshold parameter in fracture mechanics, landslide, and avalanche modeling, these findings have valuable practical implications. Specifically, the ability to accurately predict when chaos emerges while the rectangle still preserves positive dimensions enables early warning and strategic interventions in these applications, where chaotic transitions often indicate critical failure modes or abrupt natural hazard events. Thus, this work robustly connects the theoretical framework of geometric chaos with applied fields reliant on Cheeger constants for stability and safety assessments. By avoiding ensemble averaging, the framework achieves high computational efficiency and precision while maintaining theoretical rigor. The adaptability of this approach further positions it for extensions to anisotropic domains, coupled systems, and broader nonlinear dynamical contexts.

The two numerical illustrations reinforce these findings. In the first case, with $n = 5$, $m = -1$, $p = -2$, and $q = 3$, the system exhibits chaos onset at $t = 0.2383$, confirming that the sufficient conditions yield a positive Lyapunov exponent before dimensional collapse. In the second case, with $n = 3$, $m = -1$, $p = -2$, and $q = 2$, the onset occurs at $t = 0.2494$, showing how dimensional growth and decay rates interact while preserving chaos criteria. In both scenarios, the

exponential divergence of nearby trajectories confirms sensitive dependence on initial conditions and provides compelling evidence of chaotic behavior. These results highlight not only the sufficiency of the analytic conditions but also the robustness of the chaotic mechanism under parameter variation.

The present work therefore establishes a rigorous and explicit sufficient condition, $m < 0$ and $q > m$, linking geometric evolution directly to chaos onset in the classical Cheeger problem for rectangular domains. By deriving an analytic formula for the maximal Lyapunov exponent, it provides deterministic predictability and rare, precise estimates for chaos emergence at finite times ($t \approx 0.2383$ and $t \approx 0.2494$). This contribution has concrete and verified practical applications, particularly in fields such as fracture mechanics, landslide, and avalanche modeling, where the Cheeger set represents the weakest region of a structure and the Cheeger constant serves as a critical threshold parameter. Accurately predicting when chaos arises as characterized by positive Lyapunov exponents while the domain maintains positive dimensions ensures that structural integrity is preserved up to critical intervention times. These insights enable early warning and mitigation strategies in real-world scenarios where chaotic transitions often coincide with sudden failure modes or hazardous events. Thus, this work substantially bridges theoretical geometric chaos with applied disciplines that rely on stability analysis, enhancing predictive capabilities and control frameworks in complex dynamic systems.

In conclusion, this research establishes a rigorous, deterministic foundation for studying chaotic dynamics in the Cheeger problem, unifying theoretical development, numerical validation, and practical relevance. By identifying explicit sufficient conditions for chaos, deriving maximal Lyapunov exponents analytically, and quantifying finite-time transitions, it advances our understanding of sensitive geometric dynamics while providing concrete predictive capabilities. The broader impact lies in bridging geometric optimization with chaos theory to address critical challenges in engineering, materials science, geophysics, and beyond, thereby opening new avenues for predictive control and innovative applications in complex dynamical systems.

8.2 *Future directions and potential extensions*

Building on the established sufficient condition $m < 0$ and $q > m$ linking geometric evolution to chaos onset in the Cheeger problem for rectangles, and the determination of minimum chaos transition times $t \approx 0.2383$ and $t \approx 0.2494$, future research can pursue several concrete directions. One major avenue is to extend the deterministic analytic framework to non-rectangular and anisotropic shapes, examining how geometric complexity alters chaos thresholds and dynamical behavior. Another involves coupling geometric chaos criteria with multi-physical fields such as stress, temperature, or fluid dynamics to model more realistic systems like smart materials or biomechanics. Developing multi-parameter Lyapunov exponents and multi-dimensional chaos measures will provide deeper insights into system stability under coupled influences. Moreover, embedding these analytic methods into real-time monitoring and control systems can revolutionize adaptive hazard forecasting in landslides, fracture detection, and medical image stabilization by enabling precise intervention timing based on minimum chaos onset. Finally, integrating these theoretical advances with chaos-informed global optimization heuristics has the potential to enhance search efficiency and control in complex geometric optimization problems. These directions leverage the concrete minimum time results to synchronize theoretical exploration with practical predictability and control in multi-disciplinary engineering and scientific domains.

Author contributions

All authors contributed equally to the conception and design of this study. They jointly developed the methodology, carried out the analysis, and interpreted the results. The manuscript was written and revised collaboratively by all authors.

Acknowledgment

The authors gratefully acknowledge the academic environment and resources that supported the completion of this research. No external collaborators or institutions were involved in the work. The research was conducted independently by the authors.

Funding

This research did not receive any specific grant from funding agencies in the public, commercial, or not-for-profit sectors. All costs associated with the study were borne by the authors. The work reflects the authors' independent efforts without financial assistance.

Data availability statement

The present research work is entirely theoretical in nature and does not involve the collection or generation of new experimental data. As the study focuses on conceptual analysis, literature review, and theoretical frameworks, it does not contribute new empirical data that would typically require sharing or dissemination. Therefore, the template where data sharing is marked as not applicable has been chosen. This decision aligns with the nature of the research, as it emphasizes theoretical exploration rather than data-driven findings, justifying the absence of data sharing in this context.

Ethics

The authors confirm that there are no ethical concerns associated with this study. No human participants, animals, or sensitive data were involved in the research. The manuscript is an original work and complies with standard publication ethics.

Conflict of interest

The authors declare no competing financial interest.

References

[1] Reichl LE. *The Transition to Chaos*. Heidelberg: Springer; 2021. Available from: https://doi.org/10.1007/978-3-030-63534-3.

[2] Emma W. Visualizing the invisible: Performing chaos theory. *Leonardo*. 2021; 54(3): 289-293.

[3] Levy JS, Subak TF, Armstrong I, King I, Kuang L, Kuentz L, et al. Martian chaos terrain fracture geometry indicates drainage and compaction of laterally heterogeneous confined aquifers. *Icarus*. 2025; 426: 116377. Available from: https://doi.org/10.1016/j.icarus.2024.116377.

[4] Cairano LD, Gori M, Pettini G, Pettini M. Hamiltonian chaos and differential geometry of configuration space time. *Physica D: Nonlinear Phenomena*. 2021; 422: 132909. Available from: https://doi.org/10.1016/j.physd.2021.132909.

[5] Moroni G, Syam WP, Petrò S. Comparison of chaos optimization functions for performance improvement of fitting of non-linear geometries. *Measurement*. 2016; 86: 79-92. Available from: https://doi.org/10.1016/j.measurement.2016.02.045.

[6] Mahjani MG, Moshrefi R, Sharifi-Viand A, Taherzad A, Jafarian M, Hasanlou F, et al. Surface investigation by electrochemical methods and application of chaos theory and fractal geometry. *Chaos, Solitons & Fractals*. 2016; 91: 598-603. Available from: https://doi.org/10.1016/j.chaos.2016.08.011.

[7] Bazaikin YV, Galaev AS, Zhukova NI. Chaos in Cartan foliations. *Chaos*. 2020; 30(10): 103116. Available from: https://doi.org/10.1063/5.0021596.

[8] Arous BG, Subag E, Zeitouni O. Geometry and temperature chaos in mixed spherical spin glasses at low temperature: The perturbative regime. *Communications on Pure and Applied Mathematics*. 2020; 73(8): 1732-1828. Available from: https://doi.org/10.1002/cpa.21875.

[9] Zhang Z, Wang W, Zhang LY, Zhu H. A novel chaotic map constructed by geometric operations and its application. *Nonlinear Dynamics*. 2020; 102: 2843-2858. Available from: https://doi.org/10.1007/s11071-020-06060-0.

[10] Kyurkchiev N, Zaevski T, Iliev A, Kyurkchiev V, Rahnev A. Generating chaos in dynamical systems: Applications, symmetry results, and stimulating examples. *Symmetry*. 2024; 16(8): 938. Available from: https://doi.org/10.3390/sym16080938.

[11] Alexan W, Elkandoz MT, Mashaly M, Azab E, Aboshousha A. Color image encryption through chaos and KAA map. *IEEE Access*. 2023; 11: 11541-11554. Available from: https://doi.org/10.1109/ACCESS.2023.3242311.

[12] Cheeger J. A lower bound for the smallest eigenvalue of the Laplacian. In: Cunning RC. (ed.) *Problems in Analysis: A Symposium in Honor of Salomon Bochner*. Princeton, NJ: Princeton University Press; 1970. p.195-199. Available from: https://doi.org/10.1515/9781400869312-013.

[13] Kawohl B, Lachand-Robert T. Characterization of Cheeger sets for convex subsets of the plane. *Pacific Journal of Mathematics*. 2006; 225(1): 103-118. Available from: https://doi.org/10.2140/pjm.2006.225.103.

[14] Lachand-Robert T, Oudet E. Minimizing within convex bodies using a convex hull method. *SIAM Journal on Optimization*. 2005; 16(2): 368-379. Available from: https://doi.org/10.1137/040608039.

[15] Parini E, Saracco G. Optimization of the anisotropic Cheeger constant concerning the anisotropy. *Canadian Mathematical Bulletin*. 2023; 66(3): 1030-1043. Available from: https://doi.org/10.4153/S0008439523000152.

[16] Bobkov V, Parini E. On the Cheeger problem for rotationally invariant domains. *Manuscripta Mathematica*. 2021; 166: 503-522. Available from: https://doi.org/10.1007/s00229-020-01260-9.

[17] Pratelli A, Saracco G. Cylindrical estimates for the Cheeger constant and applications. *Journal of Pure and Applied Mathematics*. 2025; 194: 103633. Available from: https://doi.org/10.1016/j.matpur.2024.103633.

[18] Krejcirik D, Pratelli A. The Cheeger constant of curved strips. *arXiv:1011.3490*. 2010. Available from: https://doi.org/10.48550/arXiv.1011.3490.

[19] Leonardi GP, Neumayer R, Saracco G. The Cheeger constant of a Jordan domain without necks. *Calculus of Variations and Partial Differential Equations*. 2017; 56: 164. Available from: https://doi.org/10.1007/s00526-017-1263-0.

[20] Parini E. An introduction to the Cheeger problem. *Surveys in Mathematics and Its Applications*. 2011; 6: 9-22.

[21] Ionescu IR, Lachand-Robert T. Generalized Cheeger sets related to landslides. *Calculus of Variations and Partial Differential Equations*. 2005; 23: 227-249. Available from: https://doi.org/10.1007/s00526-004-0300-y.

[22] Ionescu IR, Lupacu-Stamate O. Boundary variation method for the generalized Cheeger problem. *Applied Numerical Mathematics*. 2019; 140: 199-214. Available from: https://doi.org/10.1016/j.apnum.2019.02.002.

[23] Pratelli A, Saracco G. On the generalized Cheeger problem and an application to 2D strips. *Revista Matemática Iberoamericana*. 2017; 33(1): 219-237. Available from: https://doi.org/10.4171/RMI/934.

[24] Georgiou GC, Huilgol RR. Cheeger sets and the minimum pressure gradient problem for viscoplastic fluids. *Journal of Non-Newtonian Fluid Mechanics*. 2023; 313: 104999. Available from: https://doi.org/10.1016/j.jnnfm.2023.104999.

[25] Froyland G, Rock CP. Higher Cheeger ratios of features in Laplace-Beltrami eigenfunctions. *Applied and Computational Harmonic Analysis*. 2025; 74: 101710. Available from: https://doi.org/10.1016/j.acha.2024.101710.

[26] Ruiz PA, Baudoin F. Korevaar-Schoen p-energies and their Γ limits on Cheeger spaces. *Nonlinear Analysis*. 2025; 256: 113779. Available from: https://doi.org/10.1016/j.na.2025.113779.

[27] Demengel F. On some nonlinear equation involving the 1-Laplacian and trace map inequalities. *Nonlinear Analysis: Theory, Methods & Applications*. 2002; 48: 1151-1163.

[28] Kawohl B, Fridman V. Isoperimetric estimates for the first eigenvalue of the p-Laplace operator and the Cheeger constant. *Commentationes Mathematicae Universitatis Carolinae*. 2003; 44(4): 659-667.

[29] Davidchack R, Lai YC. Characterization of transition to chaos with multiple positive Lyapunov exponents by unstable periodic orbits. *Physics Letters A*. 2000; 270(6): 308-313. Available from: https://doi.org/10.1016/S0375-9601(00)00335-2.

[30] Strogatz SH. *Nonlinear Dynamics and Chaos: With Applications to Physics, Biology, Chemistry, and Engineering*. USA: Chapman and Hall/CRC; 2024.

[31] Dingwell JB. Lyapunov exponents. In: *Wiley Encyclopedia of Biomedical Engineering*. USA: John Wiley and Sons, Inc.; 2006. Available from: https://doi.org/10.1002/9780471740360.ebs0702.

[32] Parini E, Saintier N. Shape derivative of the Cheeger constant. *ESAIM: Control, Optimisation and Calculus of Variations*. 2015; 21: 348-358. Available from: https://doi.org/10.1051/cocv/2014018.

[33] Oueslati R, Manita G, Chhabra A, Korbaa O. Chaos game optimization: A comprehensive study of its variants, applications, and future directions. *Computer Science Review*. 2024; 53: 100647. Available from: https://doi.org/10.1016/j.cosrev.2024.100647.

[34] Yacoubi S, Manita G, Chhabra A, Korbaa O, Mirjalili S. A multi-objective chaos game optimization algorithm based on decomposition and random learning mechanisms for numerical optimization. *Applied Soft Computing*. 2023; 144: 110525. Available from: https://doi.org/10.1016/j.asoc.2023.110525.

[35] Romanenko O. On the application of one-dimensional dynamics in the study of infinite-dimensional dynamical systems and modeling of the distributed chaos. *Ukrainian Mathematical Journal*. 2025; 76: 2038-2062. Available from: https://doi.org/10.1007/s11253-025-02436-w.

[36] Nadeem M, Arqub OA, Ali AH, Neamah HA. Bifurcation, chaotic analysis and soliton solutions to the (3 + 1)-dimensional *p*-type model. *Alexandria Engineering Journal*. 2024; 107: 245-253. Available from: https://doi.org/10.1016/j.aej.2024.07.032.

[37] Kushwaha PK, Mishra LN. A dynamic study of the generalized Cheeger problem: An application to the temporal prediction of landslides and rainfall threshold. *Sigma Journal of Engineering and Natural Sciences*. 2025; 43(3): 999-1013. Available from: https://doi.org/10.14744/sigma.2025.00087.

[38] Nehi HM, Saljooghi FH, Rahimi A, Rathour L, Mishra LN, Mishra VN. Data envelopment analysis with imprecise data: Fuzzy and interval modeling approaches. *Results in Control and Optimization*. 2025; 19: 100531. Available from: https://doi.org/10.1016/j.rico.2025.100531.

[39] Rathour L, Obradovic D, Mishra LN, Khatri K, Mishra VN. Application of the function in basic mathematics. *International Journal of Advanced Science and Engineering*. 2023; 9(4): 3144-3150. Available from: https://doi.org/10.29294/IJASE.9.4.2023.3144-3150.

[40] Sharma MK, Bhargava AK, Kumar S, Rathour L, Mishra LN, Pandey S. A fermatean fuzzy ranking function in optimization of intuitionistic fuzzy transportation problems. *Advanced Mathematical Models and Applications*. 2022; 7(2): 191-204.

[41] Sharma MK, Dhiman N, Mishra LN, Mishra VN, Sahani SK. Mediative fuzzy extension technique and its consistent measurement in the decision making of medical application. *Mathematical Problems in Engineering*. 2021; 2021: 5530681. Available from: https://doi.org/10.1155/2021/5530681.

[42] Sonker S, Munjal A, Mishra LN. Approximation of a function belonging to $Lip(\alpha, \theta, w)$ by $(C, 1)(E, q)$. *The Nepali Mathematical Sciences Report*. 2020; 37(1-2): 80-85. Available from: https://doi.org/10.3126/nmsr.v37i1-2.34095.

[43] Sharma MK, Kamini, Dhiman N, Mishra VN, Rosales HG, Dhaka A, et al. A fuzzy optimization technique for multi-objective aspirational level fractional transportation problem. *Symmetry*. 2021; 13(8): 1465. Available from: https://doi.org/10.3390/sym13081465.

[44] Mashuri A, Adenan NH, Abd Karim NS, Tho SW, Zeng Z. Application of chaos theory in different fields: A literature review. *Journal of Science and Mathematics Letters*. 2024; 12(1): 92-101. Available from: https://doi.org/10.37134/jsml.vol12.1.11.2024.

[45] Castillo JC. Differential equations: Fundamentals, solution methods, and applications in dynamical systems and chaos theory. *Ibero Sciences-Scientific and Academic Journal*. 2025; 4(2): 22-42. Available from: https://doi.org/10.63371/ic.v4.n2.a36.

[46] Matuszak M, Röhrs J, Isachsen PE, Idanovi M. Uncertainties in the finite-time Lyapunov exponent in an ocean ensemble prediction model. *Ocean Science*. 2025; 21(1): 401-418. Available from: https://doi.org/10.5194/os-21-401-2025.

[47] Caligiuri A, Eguiluz VM, Di Gaetano L, Galla T, Lacasa L. Lyapunov exponents for temporal networks. *Physical Review E*. 2023; 107(4): 044305. Available from: https://doi.org/10.1103/PhysRevE.107.044305.

[48] Nabil H, Hamaizia T. Effect of chaos on the performance of spider wasp meta-heuristic optimization algorithm for high-dimensional optimization problems. *Mathematical Modelling and Numerical Simulation with Applications*. 2025; 5(1): 143-171. Available from: https://doi.org/10.53391/mmnsa.1571964.